Formulation of epoxy-polyester powder coatings containing silver-modified nanoclays and evaluation of their antimicrobial properties

Gordon Armstrong [a, b], Roibeard Thornton [a], Michael P Ryan [c], Fathima Laffir [a], Ronald J Russell [d], Tanushree Bala [a#], Christopher Keely [b*] and Ramesh Babu [b]

[a] *Materials & Surface Science Institute, University of Limerick, National Technological Park, Castletroy, Co. Limerick, Ireland.*

[b] *Materials Ireland Research Centre, School of Physics, University of Dublin, Trinity College, Dublin 2, Ireland.*

[c] *Department of Chemical & Environmental Science, University of Limerick, National Technological Park, Castletroy, Co. Limerick, Ireland.*

[d] *Moyne Institute of Preventive Medicine, University of Dublin, Trinity College, Dublin 2, Ireland.*

[#] *Present address: Department of Chemistry, University of Calcutta, 92, A.P.C. Road, Kolkata – 700009, India.*

[*] *Present address: Centre for Research on Adaptive Nanostructures and Nanodevices, University of Dublin, Trinity College, Dublin 2, Ireland.*

Corresponding author: Gordon Armstrong. Materials & Surface Science Institute, University of Limerick, Castletroy, Co. Limerick, Ireland.

Email: gordon.armstrong@ul.ie

Fax: +353-61-213529

Telephone: +353-61-213127.

This is a preprint of a manuscript published in *Polymer Bulletin*. The final publication is available at www.springerlink.com, DOI 10.1007/s00289-011-0695-5

Abstract

Current interest in antimicrobial coatings is driven by an urgent need for more effective strategies to control microbial infection. In this study, antimicrobial nanoclays were prepared by ion-exchange of sodium montmorillonite (MMT) with silver ions which have been previously reported to exhibit biocidal activity. The extent of ion exchange achieved was estimated by x-ray photoelectron spectroscopy (XPS). The silver-modified nanoclay (AgMMT) fully inhibited growth of Gram negative *Escherichia coli* DH5α (*E. coli*) over 24 hours; annealing AgMMT under typical conditions used to prepare polymer composites did not reduce its antimicrobial efficacy. However, powder coatings of AgMMT dispersed in epoxy/polyester resin exhibited no antimicrobial effect *E. coli*. This is believed to be caused by poor wetting of the polymer coating, which restricted the diffusion of silver ion from the coating.

Keywords

Nanoclay, nanocomposite, microbial infection control, epoxy, polyester, Escherichia coli.

Introduction

The current growing interest in antimicrobial coatings is driven by an urgent need for more effective strategies to control microbial infection. However, as increasing frequency of antibiotic resistance makes it ever more difficult to treat such infections, new and more effective antimicrobial strategies and materials are required. One such strategy is to break the chain of infection by incorporation of antimicrobial substances into contact surfaces. The present study investigated the benefits of introducing nanoclays, modified so as to give them antimicrobial functionality, into standard powder coating formulations. The processing techniques used to prepare the coatings were chosen to be readily compatible with existing techniques and plant used in the powder coatings sector, so that the technology would be suitable for early transfer to industrial applications. Likewise, the conditions under which the nanoclay's and coatings' antimicrobial performance were tested were chosen to be representative of the actual conditions under which they would be used in service.

Diverse approaches have been taken to formulating antimicrobial surfaces, as reviewed by Lewis and Klibanov [1] and Kenawy *et al* [2]. Kenawy and co-workers summarized the basic requirements these novel biocidal materials must exhibit as follows: facile synthesis, long term stability, water insolubility, non-toxicity and broad spectrum biocidal activity over short contact times. Several authors have reviewed the use of silver compounds as biocides, including their molecular mechanisms of disinfection and resistance [3-7]. Silver combines

the advantages of low toxicity, broad-spectrum antimicrobial activities against Gram-negative and Gram-positive bacteria with minimal development of bacterial resistance [5]. Three key requirements must be met to achieve antimicrobial activity using silver: the metal ion must be able to react with a biomolecule within the target microbe, this ion must be accessible to the biomolecule, and the environment must be such (temperature, pH, chemicals present) that the ion's reactivity is not adversely affected. The efficacy of silver is not sensitive to the ion used. All silver salts are bactericidal, though the biocidal action of products containing silver has been directly related to the amount and rate of silver released [5,6].

Lewis and Klibanov [1] considered the rational design of sterile surface materials, using long-chain polymers functionalised with antimicrobial agents and attached to solid surfaces. They concluded that the mechanism of action of these sterile surfaces was similar to that of quaternary ammonium cations, i.e.: they disrupt the cell membrane. The flexible polymers were believed to reach across the microbial cell envelope, delivering the active moiety into the membrane and killing the pathogen.

Nanoclays have been widely studied as carriers for silver as a route to preparing antimicrobial agents [8-15]; these silver-modified nanoclays have demonstrated good antimicrobial performance against a wide range of bacteria in contact times under 12 hours. Of particular relevance to the present study, Keller-Besrest *et al* conducted a structural investigation of silver-added montmorillonite clay for possible use in the treatment of burns using EXAFS spectroscopy [8]. The silver modification was achieved by stirring the clay in a solution of silver nitrate; approximately 1 wt% of the silver available in solution was fixed by the clay. Silver ions were found to be present in the modified clay in two oxidation states: Ag^0 and Ag^+. The silver ions formed triangular clusters and were adsorbed reversibly onto the clay; 60-90 % of the ions fixed during modification were subsequently released.

In an alternative approach to achieving antimicrobial nanocomposite coatings, Kumar *et al* [16] prepared antimicrobial paints based on vegetable oil in which silver nanoparticles were embedded using a one-step process. Glass coated with this paint exhibited excellent antimicrobial properties against both *Staphylococcus aureus (S. aureus)* and *Escherichia coli (E. coli)* bacteria. Rai *et al* [17] reviewed recent advances in the use of silver nanoparticles as antimicrobial agents, comparing the proposed mechanisms of antimicrobial activity for silver nanoparticles with metallic silver, silver ions and silver zeolites.

As may be seen from the preceding overview, existing methods to achieve antimicrobial polymers largely depend on synthesising and processing a new material. For the present study, montmorillonite (MMT) nanoclays modified with silver ions were selected as MMT is

already well-known in formulation of polymer composites and coatings, and Ag exhibits broad antimicrobial activity. As silver-modified montmorillonite (AgMMT) is a polar nanoclay, it may be expected to disperse satisfactorily in polar polymer matrices only. Therefore, an epoxy/polyester matrix was selected to prepare the powder coatings. The effect of adding titania to the coating formulation was also investigated, as TiO_2 is widely used as a pigment in polymer and coatings products.

Experimental

Silver-modified nanoclay (AgMMT)

A slurry of 10.0 g Cloisite Na (Southern Clay Products; cation exchange coefficient (CEC) 92 meq/100 g) was prepared in 1 litre of hot (60 ºC) deionised water. A solution of 25% excess $AgNO_3$ (Aldrich), calculated from the CEC of the clay, was prepared in hot water/ethanol, then added to the clay slurry in portions. After stirring for 5 hours at 60 ºC, the modified nanoclay was recovered by spinning at 4600 rpm for 120 minutes on a Heittich Rotanta 460R centrifuge. The nanoclay was washed twice, by re-suspending it in deionised water with stirring for one hour followed by centrifuging, until the supernatant tested negative for nitrate ion. Finally, the nanoclay was oven-dried overnight, then ground and sieved to pass through a 180 micron sieve.

Powder coatings

A commercial formulation containing equal parts epoxy and polyester resins was used to prepare the powder coatings. 2 wt% of antimicrobial nanoclays was incorporated in each coating. Control coatings that did not contain nanoclay was also prepared. The formulations prepared are summarised in Table 1. Before use, the nanoclays were passed through a 125 micron sieve to avoid aggregation during processing. The ingredients were mixed in a shaken air bag, then extruded on a twin-screw PRISM TSC system (hopper temperature 65 ºC, barrel temperature 110 ºC, 300 rpm). After grinding to pass through a 125 micron sieve, the resulting powder was applied to a mild steel substrate using an electrostatic spray-gun and oven-cured at 180 ºC for 10 minutes. Two test panels were prepared for each nanoclay formulation.

TABLE 1

X-ray powder diffraction (XRD)

XRD patterns were collected on a Philips XPert PRO MPD diffractometer fitted with a Cu Kα radiation source. Nanoclays were passed through a 120 micron sieve and deposited on zero-background discs. 1 cm^2 coupons of powder coatings were mounted on zero-background discs. A step size of 0.015 º 2θ and collection time of 0.11 º/s was used for all experiments. Nanoclay gallery spacings, calculated from Bragg's law, were reproducible to ± 0.1 Å.

X-ray photoelectron spectroscopy (XPS)

XPS was performed on a Kratos AXIS 165 spectrometer using monochromatic Al Kα radiation of energy 1486.6 eV. High resolution spectra of Ag 3d were taken at pass energy of 20 eV, 0.05 eV step size and 100 ms dwell time per step. Surface charge was efficiently neutralised by flooding the sample surface with low energy electrons. The C 1s peak at 284.8 eV was used as a charge reference to determine core level binding energies.

Transmission electron microscopy (TEM)

TEM was conducted on a JEOL model 2011 instrument operated at an accelerating voltage of 200 kV. Samples of the powder coatings were prepared by scraping the sample with a scalpel and placing the scrapings on carbon-coated copper grids.

Antimicrobial testing

The antibacterial activity of the as-prepared nanoclay, annealed nanoclay and epoxy-polyester coating was evaluated against Gram negative E. coli, DH5α.

Optical density method

Overnight, *E. coli* culture was sub-cultured (1:20) into fresh Luri Bertani (LB) broth containing nanoclay or a disc of powder coated steel (9.5 mm diameter) and grown for 24 hours. A control in which no nanoclay or coating disc was added to the media was also prepared. For each sample, optical density measurements at a wavelength of 600nm (OD_{600}) were taken on a Varian Cary 100 UV-Visible spectrophotometer every 3 hours.

Agar disc-diffusion method

E. coli was grown overnight aerobically with agitation at 37ºC in LB broth. Preparation of the agar disc-diffusion plates involved seeding LB agar plates with *E. coli*. Molten agar was

poured into an agar plate and 3 discs (9.5 mm diameter) of each powder coating were embedded into the surface of the plates. Plates were left to solidify, but not completely dry, to promote leaching of silver from the discs used in the tests. Bacterial cultures (1:100 dilution) were streaked onto the surface of the agar plates using a sterile swab and incubated overnight at 37ºC. Calipers were used to measure zones of inhibition [18].

Contact angle analysis

Static contact angle measurements were conducted using a KSV Cam 200 instrument. Droplets of 6 µl of freshly deionised water were deposited on the samples using a Hamilton gastight syringe. At least six droplets were deposited on each sample, from which the average contact angle against water was calculated. Images were captured and the contact angles measured using KSV Cam2008 software.

Results and Discussion

The gallery spacing of neat NaMMT and modified AgMMT were compared by XRD, as shown in Fig. 1. A decrease in gallery spacing from 11.72 Å to 10.44 Å was observed following the silver modification. This is consistent with previous preparations of silver-containing montmorillonite reported by Magaña *et al* [11] and Valásková *et al* [15].

FIGURE 1

XPS was performed to confirm the presence of Ag in AgMMT. A low resolution survey spectra, shown in Fig. 2**Fig.** , yielded peak positions for Na, Mg, Si, Al, O, C, N and Ag which are characteristic of the silver modified nanoclay. Quantification of the survey spectra showing the relative concentrations of all elements detected is presented in Table 2. The presence of Na is indicative that not all Na^+ ions were exchanged in the preparation of AgMMT. A ratio of 4:1 was obtained for Ag:Na from quantification of the survey spectra using the ion's respective relative sensitivity factors and suggests that approximately 80 % of Na^+ ions were exchanged for Ag^+.

FIGURE 2

TABLE 2

A high resolution scan of Ag 3d (Fig. 3) is composed of a doublet corresponding to $3d_{5/2}$ and $3d_{3/2}$ and an energy separation of 6.0 eV. Ag $3d_{5/2}$ appears at a binding energy of 368.8 eV and has a full width at half maximum (FWHM) of 1.4 eV. Similar values were reported previously by Magaña *et al*. for silver-modified montmorillonite [11]. However, silver appears shifted to higher binding energies relative to Ag^0 and Ag^+ state [19], and the peaks observed had a broader FWHM. These observations suggested that silver incorporated in the nanoclay was present in a disordered local environment.

FIGURE 3

Having exhibited satisfactory antimicrobial properties and thermal stability, AgMMT was incorporated into a commercially available powder coating formulation to assess its usefulness in preparing antimicrobial nanocomposites. As discussed earlier, coatings were formulated both with and without TiO_2 pigment added. Control coating that did not contain nanoclay were also prepared. The formulations prepared are summarised in Table 1.
The extent of intercalation of polymer into the nanoclay galleries achieved during preparation of the powder coatings was also examined by XRD, as shown in Fig. 4. No difference was observed between the diffraction patterns obtained for samples A (control) and B (2 WT% AgMMT). Most probably, any peak attributable to AgMMT – present at 2 wt% in sample B- was masked by the contribution to the pattern from the 30 wt% of TiO_2 present. In contrast, the diffraction pattern for sample D – containing 2 wt% AgMMT and no TiO_2 – featured a shoulder at low Bragg angles not observed for control sample C, but no other peaks were observed. This indicated that AgMMT was exfoliated in the epoxy/polyester matrix of sample D, as the diffraction peak indicative of intercalated nanoclay is lost once the gallery spacing exceeds 80 Å or the nanocomposite becomes disordered [20,21]. Therefore, high-resolution transmission electron microscopy (TEM) was conducted alongside XRD on the powder coating samples B and D that contained nanoclay to confirm the degree of intercalation or exfoliation achieved.

FIGURE 4

TEM analysis of the powder coating samples was found to be in good agreement with the XRD results. The images obtained for samples B and D are presented in Fig. 5. Sample B showed good exfoliation of AgMMT within the matrix. It may be seen from Fig. 5i that the

clay platelets were well dispersed. Examination of the same region at higher magnification revealed individual clay dispersed in the matrix (Fig. 5ii). For sample D, AgMMT appeared to be very well dispersed in the matrix when observed at low magnification (Fig. 5iii). Some intercalation was visible at higher magnification as seen in Fig. 5iv. These findings are consistent with the diffraction pattern observed for sample D.

FIGURE 5

To test the effect of typical processing conditions used to prepare powder coatings on the nanoclays, a sample of AgMMT was annealed at 180 ºC for 10 minutes under ambient atmosphere. No thermal degradation of the Ag-MMT was observed after annealing. Taking the CEC of Cloisite NA to be 92 meq/100, of which approximately 80 % were calculated to have been exchanged for Ag^+ by XPS analysis, the Ag^+ content of the modified AgMMT was estimated to be 7.36×10^4 ppm. Upon incorporating this nanoclay into the polymer coating formulation at a loading of 2 wt%, the Ag^+ content of the final coating was estimated to be 8.83×10^3 ppm. For comparison, the concentration of silver required for antimicrobial efficacy has been reported as 0.1 ppb by Wohrmann and Munstedt [22].
The antimicrobial efficacy of both neat and annealed AgMMT was evaluated by monitoring OD_{600} of *E. coli* sub-cultures over 24 hours. AgMMT was found to exhibit comparable antimicrobial performance against Gram negative *E. coli* before and after annealing, as may be seen from the optical density plot shown in Fig. 6i; the sub-cultures are shown after 24 hours in Fig. 6ii.

FIGURE 6i
FIGURE 6ii

The antimicrobial activity of the powder coating samples was evaluated using the disc diffusion assays, chosen so that the test conditions would be as representative of the actual service conditions foreseen for the coatings as possible. During these assays, no antimicrobial activity was observed against *E. coli* for any of samples A – D. Representative photographs of the test discs on the agar plates are shown in Fig. 7. Zones of inhibition with an average diameter of 42 mm were observed for control samples, prepared by applying 10 μL of chloroamphenicol solution to discs of control sample C (unfilled powder coating).

FIGURE 7

It was considered possible that the absence of antimicrobial activity during the disc diffusion assays was caused by insufficient contact between the discs and the bacterial lawn, or by insufficient wetting of the coating surface. Either of these situations could impede the release of silver ions from the coating. It was also hypothesised that the TiO_2 present in the base coating formulation of samples A and B may have masked any antimicrobial activity of the functionalised nanoclays, either by exhibiting antioxidant action or by adsorbing silver ions as they were released from the surface of the samples.

Therefore, a second antimicrobial activity assay was undertaken for samples C and D; these coatings were selected because they contained only AgMMT, removing the potential for interference from TiO_2. OD_{600} of *E. coli* sub-cultures into which 9.5 mm diameter discs of samples C and D were placed was monitored over 24 hours. This experimental design was chosen to facilitate complete wetting of the coated surface and leaching of any silver ions present. However, after 24 hours, no reduction in optical density was observed for the powder coatings with respect to the bacterial control sample, as may be seen from Fig. 8.

FIGURE 8

As discussed above, adequate wetting of the coating surface would be required to allow the release of Ag^+ ions from the coating and their diffusion into the microbial cells. Hence, contact angle analysis of the coating samples A, C and D against water was conducted using the sessile drop technique to establish the wettability of the unfilled base coating and coatings containing TiO_2 or AgMMT.

When placed on a flat, horizontal solid surface, most liquids do not wet the surface fully but rather form a drop, which has a contact angle θ between the liquid and solid phases. A liquid is considered to wet a surface if $\theta < 90$ º; lower values of θ indicate better wetting of the substrate's surface. Two surfaces may be considered to have different wettability if θ differs by more than 5 º [23,24].

Table 3 shows the results of these contact angle analyses. Each value quoted was obtained using the average of at least six consistent measurements. Within the limits of experimental error, all four samples tested were found to exhibit comparable contact angles against water, exhibiting limited wettability. It is suggested that this limited wetting of the powder coating

by water restricted the ability of Ag^+ to diffuse from the coating. This may account for the absence of antimicrobial activity observed for the coatings despite the satisfactory antimicrobial activity exhibited by the silver-modified nanoclay from which the coatings were formulated.

TABLE 3

Conclusions

Silver-modified nanoclays were prepared by ion-exchange of sodium montmorillonite with silver nitrate. The nanoclay was found to be thermally stable after annealing at 180 ºC for 10 minutes, and exhibited antimicrobial activity against *E. coli* DH5α before and after annealing. However, powder coatings of AgMMT dispersed in epoxy/polyester resin exhibited no antimicrobial effect during optical density and disc diffusion assays. Contact angle analysis against water revealed that the epoxy/polyester coatings had limited wettability. Based on this finding, it was proposed that this limited wetting of the powder coating by water restricted the ability of Ag^+ to diffuse from the coating. Future work will address other factors that may affect the antimicrobial efficacy of such coatings, including the role played by surface roughness and surface energy of the coating, the rate of silver ion release, and the charge state of available ions once released.

Acknowledgements

We acknowledge the support of Enterprise Ireland (grant CFTD-2003-423). This work was enabled under the framework of the INSPIRE programme, funded by the Irish Government's Programme for Research in Third Level Institutions, Cycle 4, National Development Plan 2007-2013. Our thanks to Robert Gunning and Wynette Redington at for assistance with XRD measurements at Trinity College Dublin and the University of Limerick, respectively.

References

1. Lewis K, Klibanov AM (2005) Surpassing nature: rational design of sterile-surface materials. Trends in Biotechnology 23 (7):343-348. doi:10.1016/j.tibtech.2005.05.004

2. Kenawy ER, Worley SD, Broughton R (2007) The chemistry and applications of antimicrobial polymers: A state-of-the-art review. Biomacromolecules 8 (5):1359-1384. doi:10.1021/bm061150q

3. Thurman RB, Gerba CP (1988) The molecular mechanisms of copper and silver ion disinfection of bacteria and viruses. CRC Critical Reviews in Environmental Control 18 (4):295-315

4. Feng QL, Wu J, Chen GQ, Cui FZ, Kim TN, Kim JO (2000) A mechanistic study of the antibacterial effect of silver ions on Escherichia coli and Staphylococcus aureus. Journal of Biomedical Materials Research 52 (4):662-668
5. Lansdown ABG (2002) Silver I: its antibacterial properties and mechanism of action. Journal of Wound Care 11 (4):125-130
6. Butkus MA, Edling L, Labare MP (2003) The efficacy of silver as a bactericidal agent: advantages, limitations and considerations for future use. Journal of Water Supply Research and Technology-Aqua 52 (6):407-416
7. Silver S (2003) Bacterial silver resistance: molecular biology and uses and misuses of silver compounds. FEMS Microbiology Reviews 27 (2-3):341-353
8. Keller-Besrest F, Bénazeth S, Souleau C (1995) EXAFS structural investigation of a silver-added montmorillonite clay. Materials Letters 24 (1-3):17-21
9. Ohashi F, Oya A, Duclaux L, Beguin F (1998) Structural model calculation of antimicrobial and antifungal agents derived from clay minerals. Applied Clay Science 12 (6):435-445
10. Rivera-Garza M, Olguín MT, García-Sosa I, Alcántara D, Rodríguez-Fuentes G (2000) Silver supported on natural Mexican zeolite as an antibacterial material. Microporous and Mesoporous Materials 39 (3):431-444
11. Magaña SM, Quintana P, Aguilar DH, Toledo JA, Ángeles-Chávez C, Cortés MA, León L, Freile-Pelegrín Y, López T, Sánchez RMT (2008) Antibacterial activity of montmorillonites modified with silver. Journal of Molecular Catalysis A: Chemical 281 (1-2):192-199
12. Zhao D, Zhou J, Liu N (2006) Preparation and characterization of Mingguang palygorskite supported with silver and copper for antibacterial behavior. Applied Clay Science 33 (3-4):161-170
13. do Rosário JA, de Moura GBG, Gusatti M, Riella HG (2009) Synthesis of Silver-Treated Bentonite: Evaluation of its Antibacterial Properties. Paper presented at the ICheaP-9 The ninth International Conference on Chemical & Process Engineering, Rome, Italy, 10-13 May 2009
14. Ohashi F, Ueda S, Taguri T, Kawachi S, Abe H (2009) Antimicrobial activity and thermostability of silver 6-benzylaminopurine montmorillonite. Applied Clay Science 46 (3):296-299
15. Valásková M, Hundáková M, Kutláková KM, Seidlerová J, Capková P, Pazdziora E, Matejová K, Hermánek M, Klemm V, Rafaja D Preparation and characterization of antibacterial silver/vermiculites and silver/montmorillonites. Geochimica et Cosmochimica Acta 74 (22):6287-6300
16. Kumar A, Vemula PK, Ajayan PM, John G (2008) Silver-nanoparticle-embedded antimicrobial paints based on vegetable oil. Nature Materials 7 (3):236-241. doi:10.1038/nmat2099
17. Rai M, Yadav A, Gade A (2009) Silver nanoparticles as a new generation of antimicrobials. Biotechnology Advances 27 (1):76-83. doi:10.1016/j.biotechadv.2008.09.002
18. Bauer AW, Kirby WM, Sherris JC, Turck M (1966). American Journal of Clinical Pathology:493-496
19. Moulder JF, Stickle WF, Sobol PE, Bomben KD (1992) Handbook of X-Ray Photoelectron Spectroscopy. Perkin-Elmer Corporation, Eden Prairie
20. Alexandre M, Dubois P (2000) Polymer-layered silicate nanocomposites: preparation, properties and uses of a new class of materials. Materials Science and Engineering: R: Reports 28 (1-2):1-63
21. Sinha Ray S, Okamoto M (2003) Polymer/layered silicate nanocomposites: a review from preparation to processing. Progress in Polymer Science 28 (11):1539-1641
22. Wohrmann RM, Munstedt H (1998). Infection 26:49-52

23. Adamson AW (1976) The Solid-Liquid Interface - Contact Angles. In: Physical Chemistry of Surfaces, 3rd edition. John Wiley and Sons, New York, pp 333-371
24. Comyn J (1997) Contact Angles in the Study of Adhesion. In: Adhesion Science. Royal Society of Chemistry, Cambridge, pp 98-113

Figure legends

Fig. 1 XRD patterns of NaMMT (A) and AgMMT (B). Diffraction patterns are shifted vertically on the Y axis for clarity

Fig. 2 XPS survey spectrum for AgMMT

Fig. 3 High-resolution XPS spectrum of Ag 3d for AgMMT

Fig. 4 XRD patterns for powder coating samples A – D. Diffraction patterns are shifted vertically on the Y axis for clarity

Fig. 5 TEM images of (i, ii) Sample B and (iii, iv) Sample D, showing the extent of intercalation of AgMMT achieved for each formulation. The region circled in image iii is shown at higher magnification in image iv

Fig. 6 (i) Antimicrobial performance of nanoclays. Optical density (OD_{600}) of broth measured over 24 hours. ◊ Control; □ AgMMT as-prepared; Δ AgMMT annealed. (ii) Nanoclay samples after 24 hours

Fig. 7 Close-up images of agar plates from disc diffusion tests of powder coatings. (i) Sample A, (ii) Sample B, (iii) Sample C, (iv) Sample D

Fig. 8 OD_{600} of E. coli sub-cultures containing coated steel specimens from trial 2. ● Blank (growth media only) ◊ Bacterial control (no discs); □ Sample D; Δ Sample 1; ○ Sample A

Tables

Table 1 Powder coating formulations

Formulation (wt%)	A	B	C	D
Epoxy	30.00	30.00	45.00	45.00
Polyester	30.00	30.00	45.00	45.00
Processing aid	10.00	10.00	10.00	10.00
Titanium dioxide	30.00	30.00	-	-
AgMMT	-	2.00	-	2.00

Table 2 Assignment of XPS peaks for AgMMT

Element	O 1s	Si 2p	C 1s	Al 2p	Ag 3d	N 1s	Mg 2s	Na 1s
Binding energy (eV)	532.1	102.9	284.8	74.8	368.8	401.0	88.3	1072.3
Atomic %	60.8	16.0	13.4	5.9	2.0	0.8	0.7	0.5

Table 3 Water contact angles and surface energies for samples A-D

Sample	θ (º)
A	85.9 ± 6.2
C	93.6 ± 5.3
D	93.1 ± 7.8

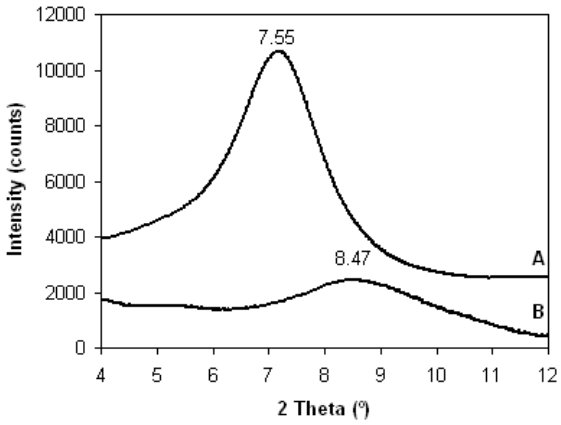
12000
10000
8000
6000
4000
2000
0
Intensity (counts)
7.55
8.47
A
B
4
5
6
7
8
9
10
11
12
2 Theta (°)

Fig 1

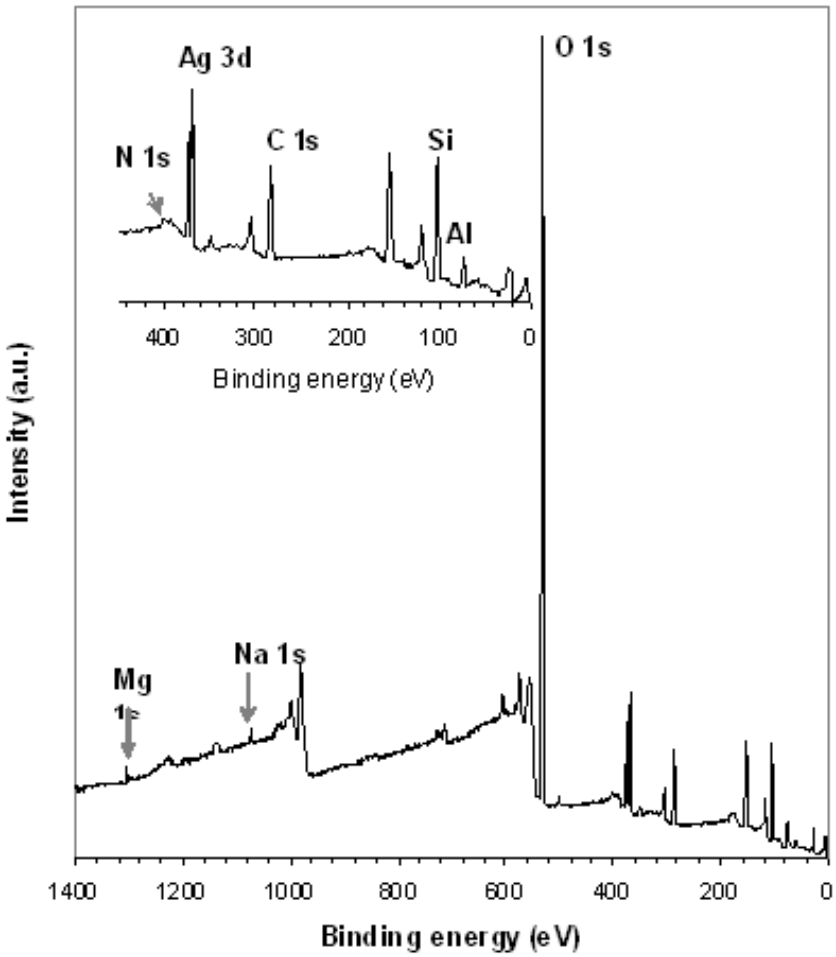
Ag 3d
O 1s
N 1s
C 1s
Si
Al
400
300
200
100
0
Binding energy (eV)
Intensity (a.u.)
Mg
Na 1s
1400
1200
1000
800
600
400
200
0
Binding energy (eV)

Fig 2

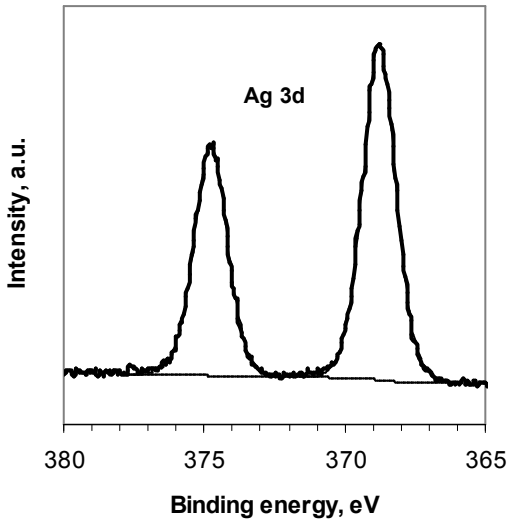

Fig 3

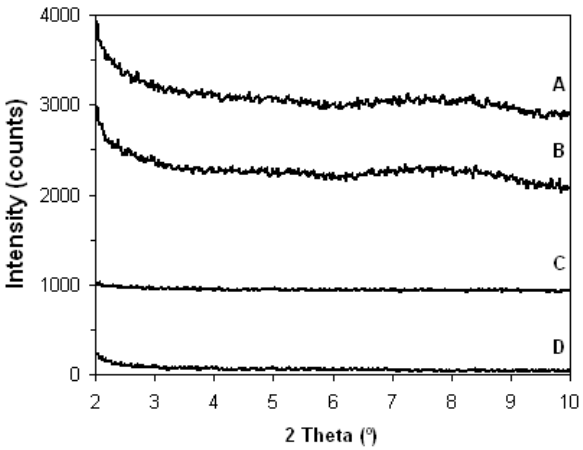
4000
3000
2000
1000
0
Intensity (counts)
2
3
4
5
6
7
8
9
10
2 Theta (°)
A
B
C
D

Fig 4

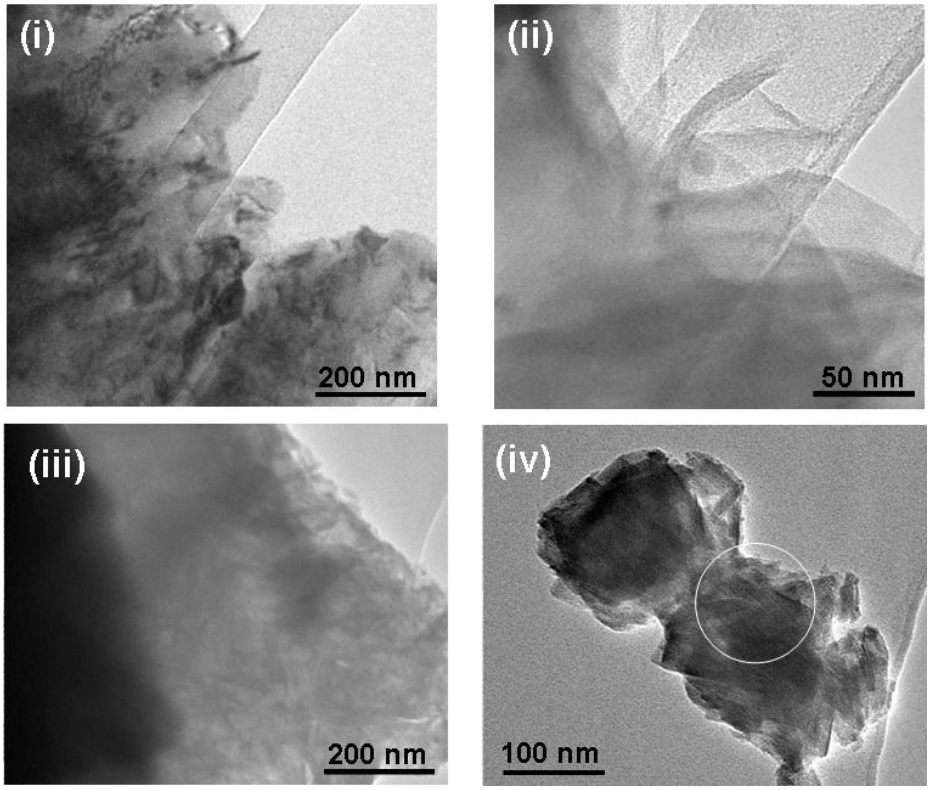

Fig 5

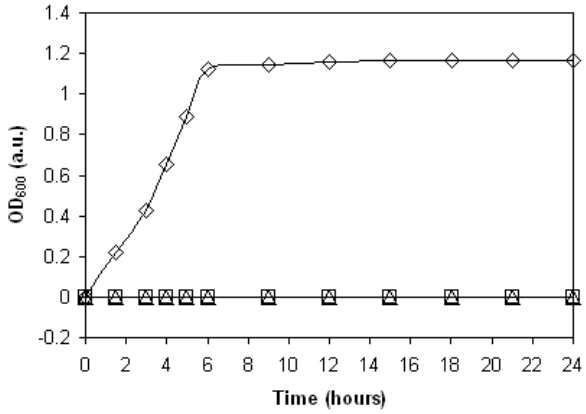
1.4
1.2
1
0.8
0.6
0.4
0.2
0
-0.2
OD600 (a.u.)
0 2 4 6 8 10 12 14 16 18 20 22 24
Time (hours)

Fig 6i

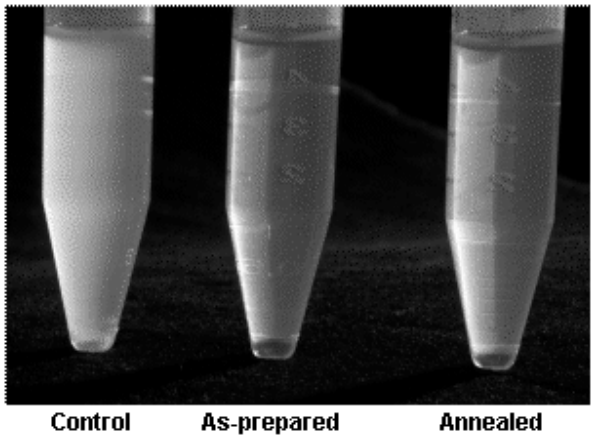

Fig 6ii

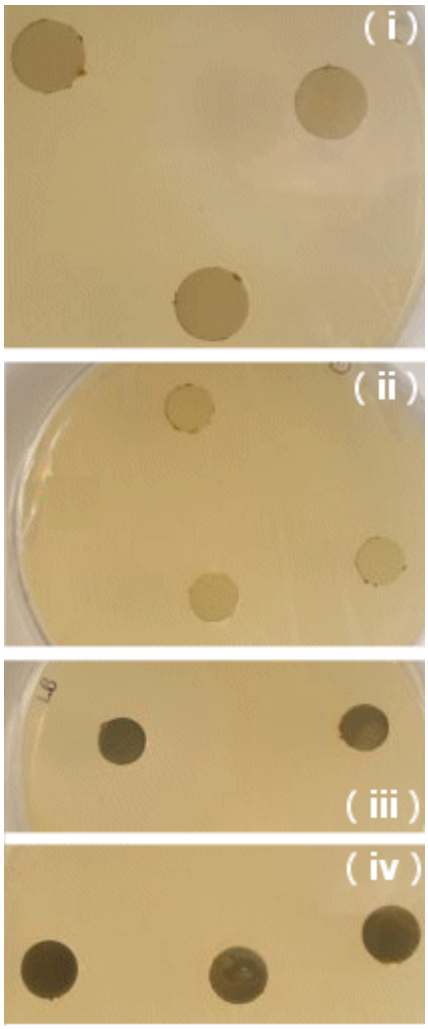

Fig 7

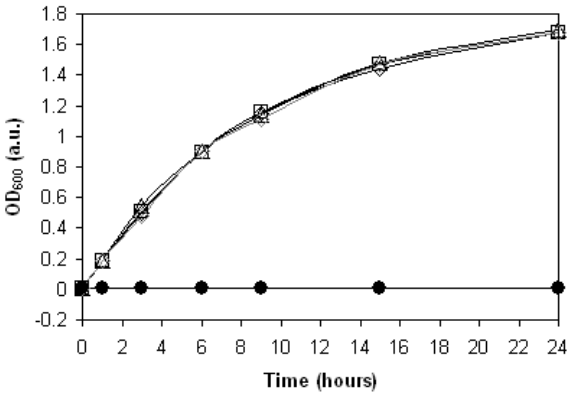
1.8
1.6
1.4
1.2
1
0.8
0.6
0.4
0.2
0
-0.2
OD600 (a.u.)
0 2 4 6 8 10 12 14 16 18 20 22 24
Time (hours)

Fig 8